Rare Metal Materials and Engineering
Volume 53, Issue 4, April 2024
Available online at www.rmme.ac.cn

Science Press

Cite this article as: Ma Xilong, Matsugi Kazuhiro, Shang Zhifeng, et al. Design of *α*-type Titanium Alloys with Improved Corrosion Resistance and Tensile Properties[J]. Rare Metal Materials and Engineering, 2024, 53(04): 947-953. DOI: 10.12442/j.issn.1002-185X.20230381.

ARTICLE

Design of α-type Titanium Alloys with Improved Corrosion Resistance and Tensile Properties

Ma Xilong[1,2], Matsugi Kazuhiro[2], Shang Zhifeng[1], Su Hongji[1], Jia Bowen[1], Nie Guoquan[3]

[1] School of Materials Science and Engineering, Shijiazhuang Tiedao University, Shijiazhuang 050043, China; [2] Department of Mechanical Materials Engineering, Hiroshima University, Higashi-Hiroshima 739-8527, Japan; [3] School of Mechanical Engineering, Shijiazhuang Tiedao University, Shijiazhuang 050043, China

Abstract: Newly designed α-type titanium (α-Ti) alloys were proposed based on both electron parameters (bonding time Bo_t and d-orbital energy level Md_t). The newly designed α-Ti alloy Ti-5Al-4Zr-3.6Sn, modified alloy Ti-5Al-3Sn-1.9Zr, and reference alloy Ti-5Al-2.5Sn have the same Bo_t value of 3.847 and different Md_t values of 2.430, 2.426, and 2.422, respectively. The ultimate tensile strength (σ_{UTS}), fracture strain (ε_f), and hot salt corrosion resistance of the three α-Ti alloys were measured. The three α-Ti alloys were produced by the cold crucible levitation melting (CCLM) technique. Results show that homogeneous microstructures can be observed in three α-Ti alloys. The α mono-phase in three α-Ti alloys has the grain size of approximately 600 μm. σ_{UTS} and ε_f of Ti-5Al-4Zr-3.6Sn alloy are 801 MPa and 16%, respectively; σ_{UTS} and ε_f of Ti-5Al-3Sn-1.9Zr alloy are 708 MPa and 15%, respectively; σ_{UTS} and ε_f of Ti-5Al-2.5Sn alloy are 603 MPa and 15%, respectively. After hot salt corrosion tests were conducted for 28.8 ks, the mass loss ratio of Ti-5Al-4Zr-3.6Sn, Ti-5Al-3Sn-1.9Zr, and Ti-5Al-2.5Sn alloys is 2.61%, 2.83%, and 3.10%, respectively. The results of σ_{UTS}, ε_f, and hot salt corrosion resistance indicate that the newly designed alloy Ti-5Al-4Zr-3.6Sn has great potential for practical applications.

Key words: alloy design; α-type titanium alloys; CCLM; tensile properties; hot salt corrosion test

α-type titanium (α-Ti) alloys normally consist of α-stabilizing elements (aluminum) and neutral elements (zirconium and tin), and they have the advantages of high specific strength, low magnetic susceptibility, high electrical resistivity, and low thermal conductivity[1–2], which are extensively used in the fields of chemical process, cryogenic usage, and the construction of offshore drilling platforms. Nevertheless, the near α-Ti alloys can react with salts in the ocean air at elevated temperatures, leading to the reduction in service life[3–4]. To expand the use of near α-Ti alloys, further development efforts should be made to enhance the mechanical strength and hot salt corrosion resistance[1,5]. It is reported that the impurities or contaminants from the crucible and atmosphere may affect the mechanical properties of Ti alloys[6–7]. It is essential to form Ti alloys with extremely low interstitial impurities to regulate their functionalities. The source of such impurities usually stems from the gaseous atmosphere of furnace and the crucible contamination. The cold crucible levitation melting (CCLM) technique can prevent any impurity seep and effectively control the furnace vacuum[8–9]. The molten metals are treated by the eddy current of CCLM technique and then melted without direct contact with the crucible materials. The speed of solidification cooling process for molten alloys can be precisely controlled by CCLM technique. Even distribution of solute elements in Ti alloys can be obtained by diffusion mixing and strong stirring induced by electromagnetic forces[10–11].

Before the proposal of d-electron concept, the design of titanium alloys basically relies on the laborious experiment trials and empirically derived rules, which has high cost and inefficient process[12]. Morinaga et al[10] calculated the bonding time Bo_t and d-orbital energy level Md_t of elements by the body-centered cubic (bcc) *M*Ti14 cluster and hexagonal close-packed (hcp) *M*Ti18 models, respectively. High temperature

Received date: June 15, 2023
Foundation item: Natural Science Foundation of Hebei Province of China (E2021210114); Project of Hebei Province Department of Human Resources and Social Security of China (C20220325)
Corresponding author: Nie Guoquan, Ph. D., Professor, School of Mechanical Engineering, Shijiazhuang Tiedao University, Shijiazhuang 050043, P. R. China, Tel: 0086-311-87936063, E-mail: niegq@stdu.edu.cn

α-type alloy and high strength β-type alloy have been developed by considering their Bo_t and Md_t values and positions in the Bo_t-Md_t diagram[13–16]. Therefore, the applications of discrete variational-Xα (DV-Xα) cluster calculation method to design binary and multi-element Ti alloys are widely used and accepted[17–18]. However, the researches on α-Ti alloys with new composition, high corrosion resistance, high mechanical performance, and low cost based on Bo_t and Md_t parameters are rarely reported.

In this research, the commercial α-Ti alloy Ti-5Al-2.5Sn was selected as the reference alloy, the modified and designed α-Ti alloys were proposed based on the Bo_t and Md_t parameters. The microstructures of three α-Ti alloys were controlled by the identical cooling and solidification conditions of CCLM technique. The reliability of DV-Xα method to design α-Ti alloy with high corrosion resistance, good mechanical performances, and low cost was verified. With the same Bo_t value, the relationship of Md_t values with tensile behavior and hot salt corrosion resistance of three α-Ti alloys was evaluated.

1 Alloy Design for α-Ti Alloys in Bo_t-Md_t Diagram

New α-Ti alloys were designed based on the Bo_t and Md_t parameters through DV-Xα method[19–20]. The content of each solute element was calculated through the cluster model of *M*Ti18 alloy and hcp Ti alloy[10,16]. The arithmetic mean values of Bo_t and Md_t of experiment alloys can be calculated by Eq.(1) and Eq.(2), respectively:

$$Bo_t=\sum X_i(Bo_t)_i \quad (1)$$

$$Md_t=\sum X_i(Md_t)_i \quad (2)$$

where X_i is the molar fraction of component i in the alloy; $(Md_t)_i$ and $(Bo_t)_i$ are the Md_t and Bo_t values of component i, respectively. The calculated results show that three experiment α-Ti alloys have the same Bo_t value of 3.847. However, the designed alloy Ti-5Al-4Zr-3.6Sn, modified alloy Ti-5Al-3Sn-1.9Zr, and reference alloy Ti-5Al-2.5Sn have different Md_t values of 2.430, 2.426, and 2.422, respectively.

2 Experiment

The raw materials used for the preparation of three experiment α-Ti alloys consisted of Ti (purity of 99.8wt%), Al (purity of 99.9wt%), Sn (purity of 98.5wt%), and Zr (purity of 98.0wt%). The ingots were manufactured by CCLM (capable production of 1 kg Fe/100+60 kW) with water-cooled copper crucible in the argon gas atmosphere with purity of 99.99%[9]. The specimens were cut directly from the ingot by wire cutting. Optical microscope (OM) was used to observe the specimen microstructure. Before OM observation, the specimens were ground by 80#–2500# sandpaper, polished, and etched by the mixture solution of distilled water, nitric acid, and hydrofluoric acid with volume ratio of 95∶3∶2. The phases of α-Ti alloys were identified by X-ray diffraction (XRD) with Cu Kα radiation (40 kV, 30 mA) at room temperature.

For the tensile specimens, the gauge size was 6.0 mm in diameter and 20.0 mm in length. The grip diameter was 10.0 mm. The tensile tests were conducted with the initial strain rate of 1.9×10^{-4} s^{-1} at room temperature in air. An extensometer was used to measure the elongation of tensile specimens. The salt corrosion resistance of three experiment α-Ti alloys was evaluated by the hot salt corrosion tests. The procedure of hot salt corrosion tests is shown in Fig.1. Hot salt corrosion test specimens were obtained by wire cutting from ingots (10 mm×5 mm×1.5 mm). Before immersion into the molten salt, all six surfaces of the specimens were ground by abrasive paper from 80# to 2000#. The molten salts used in the experiment were Na_2SO_4+45mol% NaCl, the temperature was 923 K, and the immersion duration was 28.8 ks. The mass loss was measured every 2 h in order to monitor the corrosion process. To ensure the good contact between the fused salt (Na_2SO_4+45mol% NaCl) and specimens, they were hung through the platinum wire. Subsequently, the specimens were cleaned by submersion in 9.4mol% NaOH+0.67mol% $KMnO_4$ boiling solution for 30 min to remove any solidified salt residue from the specimen surface. Then, the specimens were cleaned in 0.88mol% $(NH_4)_2HC_6H_5O_7$ boiling solution for 20 min to wash the residual salt and $KMnO_4$. Afterwards, the specimens were thoroughly rinsed and dried to remove the contaminants. Finally, the weighing process was conducted to obtain the mass loss ratio of specimens. To further investigate the mechanism of hot salt corrosion of near α-Ti alloys and the reliability of the mass loss ratio, the microstructure of hot salt corrosion layer of specimens was observed by the electron probe micro-analyzer (EPMA) after continuous immersion in hot salts for 28.8 ks.

3 Results and Discussion

3.1 Microstructure

Fig.2a–2f show OM images of three experiment α-Ti alloys. The grain sizes are approximately 600 μm in all three experiment α-Ti alloys, as shown in Fig. 2a – 2c. This phenomenon is attributed to the effect of CCLM technique with the manufacture process. The lamellar clusters with different orientations inside the grains of three experiment α-Ti alloys can be observed, as shown in Fig. 2d – 2f. The lamellar cluster structure is a distinctive feature of α-Ti alloys, resulting from the transformation from β phase to α phase during the cooling process. The two slip directions and six slip planes of the Ti unit cell provide 12 possible orientations. As indicated in the marked ovals in Fig. 2, the average layer thickness of lamellar clusters in the Ti-5Al-4Zr-3.6Sn, Ti-5Al-

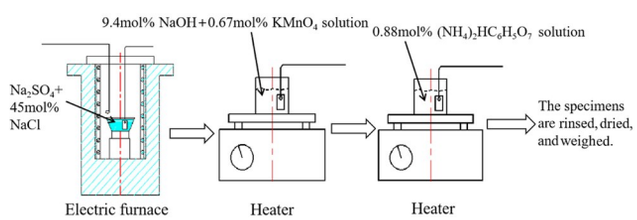

Fig.1 Schematic diagram of hot salt corrosion test

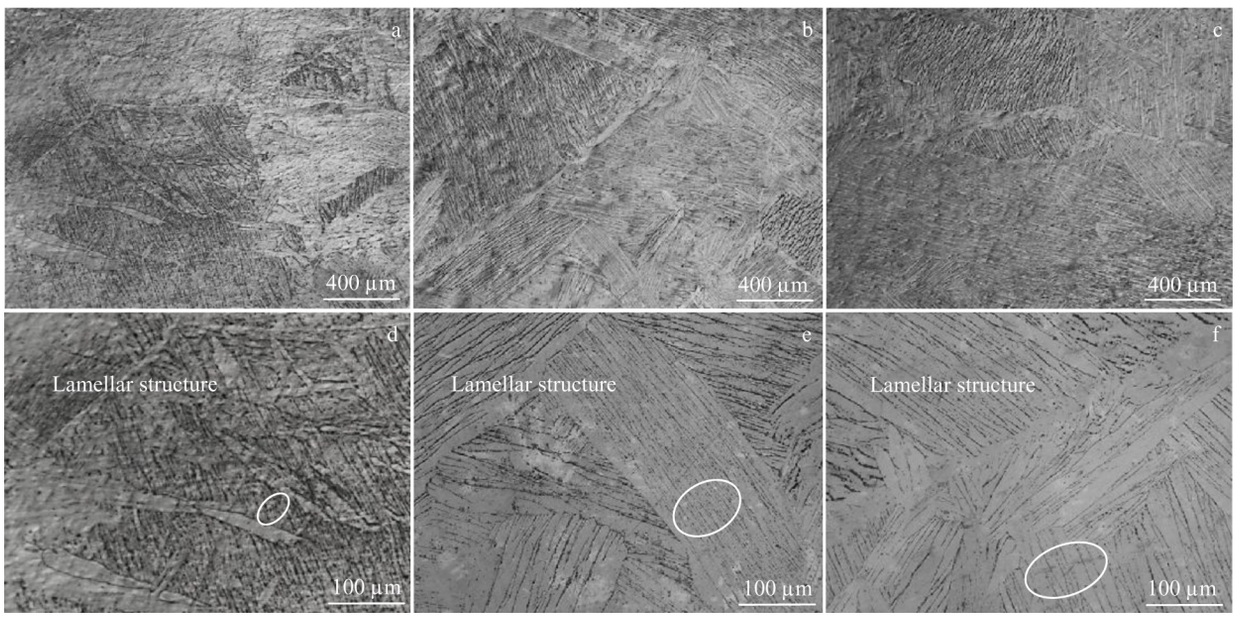

Fig.2 OM images of Ti-5Al-4Zr-3.6Sn alloy (a, d), Ti-5Al-3Sn-1.9Zr alloy (b, e), and Ti-5Al-2.5Sn alloy (c, f)

3Sn-1.9Zr, and Ti-5Al-2.5Sn alloys is 5, 8, and 10 μm, respectively. The lamellar cluster structure of the designed and modified alloys is refined, compared with that in the reference alloy, which is attributed to their distinct elemental composition. More solute elements provide more nucleation opportunities for Ti alloys, resulting in the refinement of lamellar cluster structure[21–22]. Moreover, the Ti alloys with high content of solute elements usually have high mechanical strength, excellent corrosion resistance, and fine lamellar cluster microstructure with different orientations[23–24]. The designed alloy Ti-5Al-4Zr-3.6Sn has the highest content of solute elements and it shows the optimal refined lamellar cluster microstructure among three experiment α-Ti alloys.

XRD patterns of three experiment α-Ti alloys are shown in Fig. 3. It can be seen that all alloys consist of α mono-phase. Interestingly, the designed alloy Ti-5Al-4Zr-3.6Sn has more peaks than the modified alloy Ti-5Al-3Sn-1.9Zr and the reference alloy Ti-5Al-2.5Sn do, which is attributed to different refinement degrees of the lamellar structure and the large difference in crystallographic orientations. In addition, the peak widths of three experiment α-Ti alloys are basically the same. The average layer thickness ranges from 5 μm to 10 μm, indicating that the peak width is slightly influenced. XRD results are consistent with the observation results of OM images.

3.2 Tensile properties

Fig.4 shows the tensile properties of three experiment α-Ti alloys. The ultimate tensile strength (σ_{UTS}) and fracture strain (ε_f) of the designed alloy Ti-5Al-4Zr-3.6Sn are 801 MPa and 16%, respectively; σ_{UTS} and ε_f of modified alloy Ti-5Al-3Sn-1.9Zr are 708 MPa and 15%, respectively; σ_{UTS} and ε_f of reference alloy Ti-5Al-2.5Sn are 603 MPa and 15%, respectively. The tensile properties of the designed and modified alloys are obviously improved, compared with those of the reference alloy. According to the Hall-Petch relationship, the yield stress and the flow stress of the alloys can be increased with the structure refinement[25–26]. The refined lamellar microstructure provides a more uniform

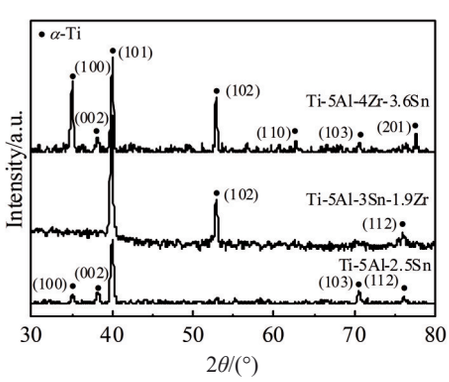

Fig.3 XRD patterns of Ti-5Al-4Zr-3.6Sn alloy, Ti-5Al-3Sn-1.9Zr alloy, and Ti-5Al-2.5Sn alloy

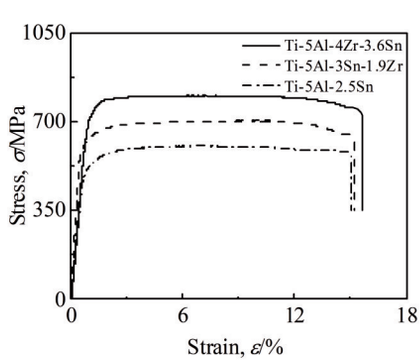

Fig.4 Stress-strain curves of Ti-5Al-4Zr-3.6Sn alloy, Ti-5Al-3Sn-1.9Zr alloy, and Ti-5Al-2.5Sn alloy

distribution of stresses during the deformation, leading to the reduced susceptibility to fatigue crack initiation and propagation[27]. Furthermore, the solid solution strengthening has contribution to the enhancement in tensile properties of alloys. The designed alloy has the highest content of additional elements, the most refined lamellar cluster structure, and the most complex lamellar orientations, therefore exhibiting the highest tensile strength. The particular chemical composition of the designed alloy Ti-5Al-4Zr-3.6Sn has great potential in the applications requiring high mechanical performance.

Fig. 5 shows the fracture appearances and magnified morphologies of the designed and reference alloys. The dimple fracture patterns appear in both α-Ti alloys at the relative satisfaction ε_f values. Fine and deep dimples with high density can be observed in the designed alloy Ti-5Al-4Zr-3.6Sn, whereas coarse voids appear in the reference alloy Ti-5Al-2.5Sn. The resistance to crack propagation and the energy absorption capacity of alloys are commonly effected by the localized plastic deformation and the growth of void or dimples[28–29]. Longer crack propagation path and more obstacles can be found in the designed alloy Ti-5Al-4Zr-3.6Sn, indicating a more effective mechanism for the energy absorption during fracture, which leads to higher tensile properties, compared with those of the reference alloy Ti-5Al-2.5Sn. This result can also be obtained from the tensile results in Fig. 4. The voids are characteristic morphology of ductile fracture and they can be observed in the reference alloy Ti-5Al-2.5Sn. The void nucleation occurs in the processes, such as inclusion fracture or decohesion at the inclusion-matrix interface. In this case, relatively hard inclusions do not deform at the same rate as that of the matrix, and the voids are formed to accommodate the incompatibility[30–31].

The Vickers hardness of three experiment α-Ti alloys are showed in Fig. 6. The Vickers hardness of Ti-5Al-4Zr-3.6Sn, Ti-5Al-3Sn-1.9Zr, and Ti-5Al-2.5Sn alloys is 3077.2, 2812.6, and 2567.6 MPa, respectively. Different contents of solute elements result in different degrees of solid solution strengthening. Additionally, the average layer thickness of the lamellar structure also plays an important role in the determination of the Vickers hardness of α-Ti alloys[30]. The designed alloy Ti-5Al-4Zr-3.6Sn with the most refined lamellar microstructure has high efficient load transfer and reduced susceptibility to deformation, resulting in improved Vickers hardness. Simultaneously, the designed alloy Ti-5Al-4Zr-3.6Sn, which contains the highest content of solute elements, exhibits the highest degree of solid solution strengthening, compared with those of other two alloys. Moreover, the variation of Vickers hardness of three experiment α-Ti alloys has similar tendency to that of tensile

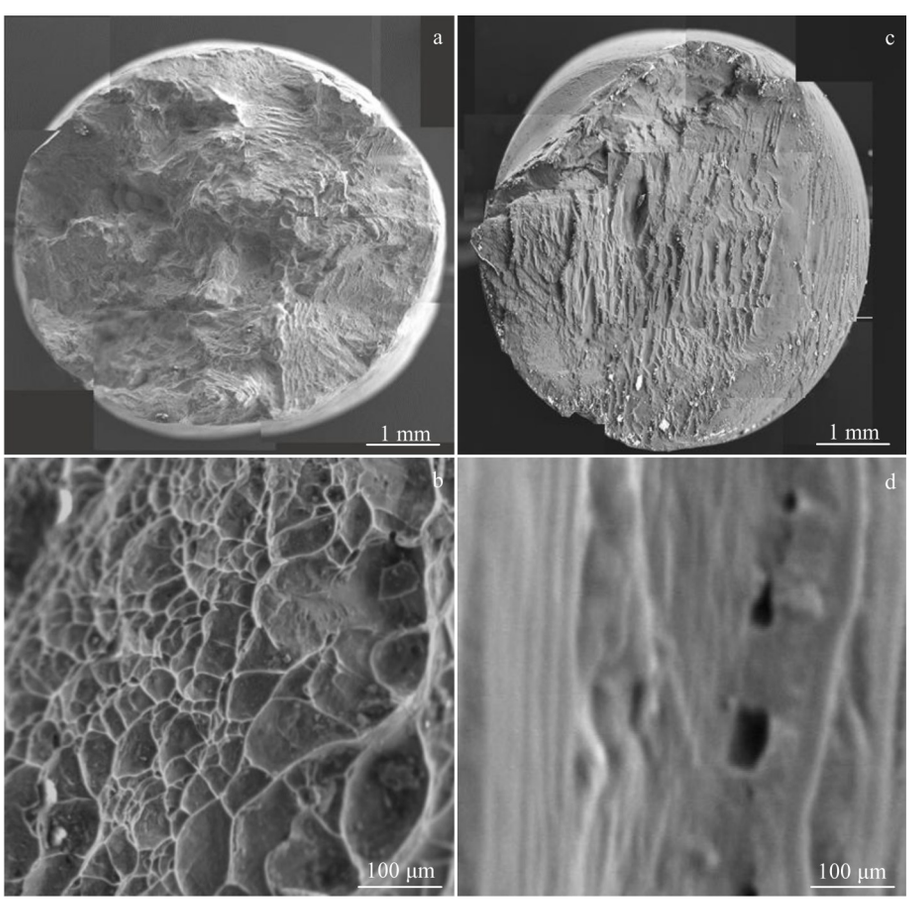

Fig.5 Fracture appearances (a, c) and magnified morphologies (b, d) of tensile specimens of Ti-5Al-4Zr-3.6Sn alloy (a–b) and Ti-5Al-2.5Sn alloy (c–d)

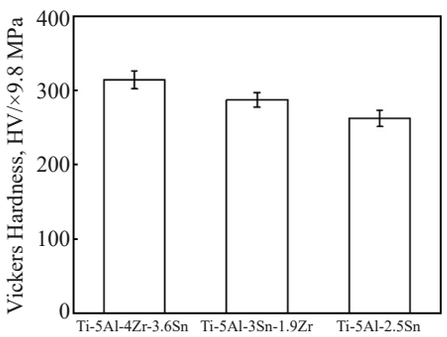

Fig.6 Vickers hardness of Ti-5Al-4Zr-3.6Sn alloy, Ti-5Al-3Sn-1.9Zr alloy, and Ti-5Al-2.5Sn alloy

results in Fig.4.

3.3 Hot salt corrosion resistance of α-Ti alloys

To evaluate the corrosion reaction degree and the mass loss of α-Ti alloys, the mass loss ratios after corrosion for 28.8 ks of three experiment α-Ti alloys are shown in Table 1. The mass loss ratio of Ti-5Al-4Zr-3.6Sn alloy, Ti-5Al-3Sn-1.9Zr alloy, and Ti-5Al-2.5Sn alloy is 2.61%, 2.83%, and 3.10%, respectively. The hot salt corrosion resistance of designed and modified alloys is greatly improved, compared with that of the reference alloy. This result indicates that the corrosion resistance is related to the solute content and refinement of lamellar microstructure[23].

In order to thoroughly investigate the mechanism of hot salt corrosion and to evaluate the dependence of mass loss ratio, the composition and EPMA mapping results (Fig. 7) of three

Table 1 Mass loss ratios of Ti-5Al-4Zr-3.6Sn alloy, Ti-5Al-3Sn-1.9Zr alloy, and Ti-5Al-2.5Sn alloy after hot salt corrosion test for 28.8 ks (%)

Alloy	Ti-5Al-4Zr-3.6Sn	Ti-5Al-3Sn-1.9Zr	Ti-5Al-2.5Sn
Mass loss ratio	2.61	2.83	3.10

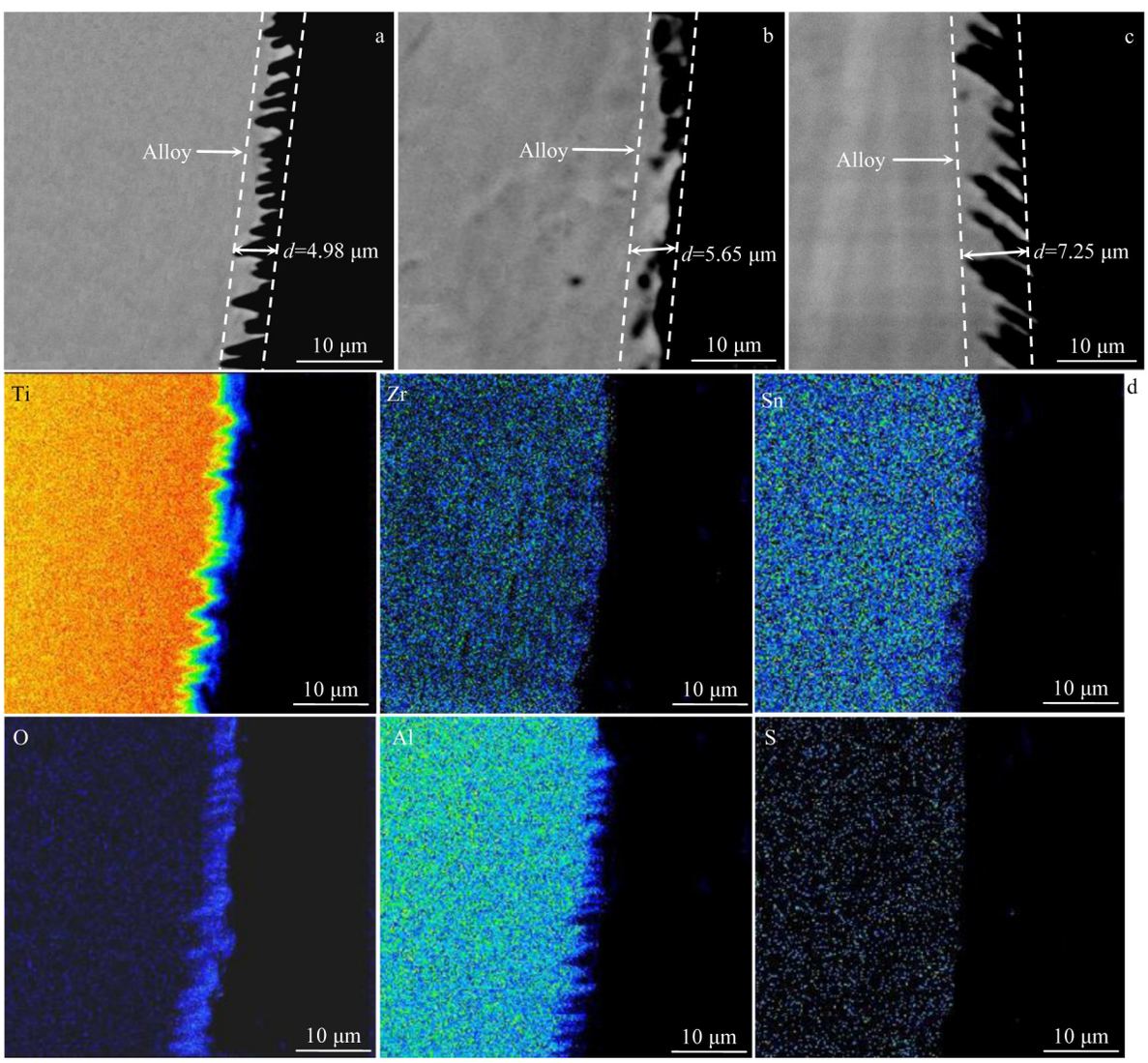

Fig.7 Cross-section morphologies of Ti-5Al-4Zr-3.6Sn alloy (a), Ti-5Al-3Sn-1.9Zr alloy (b), and Ti-5Al-2.5Sn alloy (c); EPMA mapping results of Ti-5Al-4Zr-3.6Sn alloy of Fig.7a (d)

experiment α-Ti alloys after immersion in hot salt for 28.8 ks were analyzed. The cross-section morphologies show the thickness of corrosion layers and the distribution of solute elements in alloys after hot salt corrosion test for 28.8 ks. The thicknesses of corrosion layers of the designed, modified, and reference alloys are 4.98, 5.65, and 7.25 μm, respectively. The thickness and mass loss ratio results of corrosion layers indicate that the designed alloy Ti-5Al-4Zr-3.6Sn exhibits the most impressive hot salt corrosion resistance, the thinnest corrosion layer, and the least mass loss, compared with those of the modified and reference alloys. EPMA mapping results demonstrate that no diffusion behavior of solute elements or salts can be observed in the experiment α-Ti alloys. The corrosion reactions occur at different rates on the entire contact surface between the specimens, and the fused salt is caused by the following reasons. The local electrochemical attack corresponds to the formation of jagged interfaces of specimens. Concentration-cell corrosion, namely electrochemical attack, refers to the corrosion of metal or alloy by stagnant solution with small volume[32–33]. Severe corrosion reaction occurs at the place with a small amount of ZrO_2 and Al_2O_3, where chlorine ions barely have difficulty in collision with titanium oxides. Slight corrosion occurs on the regions coated by solid corrosion products or refractory oxides which exhibit protective behavior. According to the specimen surface, a dense outer oxide layer of oxidizing products can be observed, as well as a porous inner oxide layer. The entire surface of the specimens suffers general corrosion, indicating the widespread metal loss throughout the surface. The synergistic effects of alloying elements enhance the corrosion resistance of α-Ti alloys, demonstrating the importance of alloy design and composition in enhancement of the mechanical properties and corrosion resistance of α-Ti alloys under harsh environments.

The relationships of Md_t value with σ_{UTS} and mass loss ratio of three experiment α-Ti alloys are shown in Fig.8, reflecting the tensile properties and hot salt corrosion resistance. For the three experiment α-Ti alloys with the same Bo_t value (3.487), both their σ_{UTS} and hot salt corrosion resistance are improved approximately linearly with increasing the Md_t value. For example, the difference in Md_t value between the designed alloy and the modified alloy is 0.004, and their difference in σ_{UTS} and mass loss ratio after hot salt corrosion test for 28.8 ks is 93 MPa and 0.22%, respectively. The difference in Md_t value between the modified alloy and the reference alloy is also 0.004, and their difference in σ_{UTS} and the mass loss ratio after hot salt corrosion test for 28.8 ks is 105 MPa and 0.19%, respectively. These phenomena are all attributed to the variations in the content of solute elements and the average layer thickness of three experiment α-Ti alloys, which reinforces the alloys and promotes the formation of protective oxide layer. The composition of the designed alloy Ti-5Al-4Zr-3.6Sn and modified alloy Ti-5Al-3Sn-1.9Zr can be optimized based on the Bo_t and Md_t parameters, therefore improving the mechanical properties and hot salt corrosion resistance. The consideration of d-electron concept is an effective approach for the development of new α-Ti alloys.

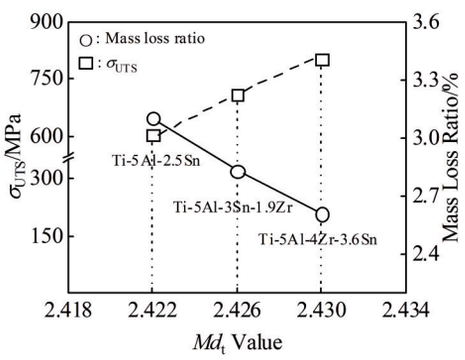

Fig.8 Relationships of Md_t value with ultimate tensile strength and mass loss ratio of Ti-5Al-4Zr-3.6Sn alloy, Ti-5Al-3Sn-1.9Zr alloy, and Ti-5Al-2.5Sn alloy

4 Conclusions

1) New designed α-Ti alloys are proposed on the basis of bonding time Bo_t and d-orbital energy level Md_t in the hcp model. Three experiment α-Ti alloys all show the α monophase with grain sizes of approximately 600 μm and present the lamellar microstructure with different orientations.

2) The designed alloy Ti-5Al-4Zr-3.6Sn shows the highest ultimate tensile strength (σ_{UTS}) of 801 MPa and fracture strain (ε_f) of approximately 16%. After hot salt corrosion test for 28.8 ks, the mass loss ratio of designed alloy Ti-5Al-4Zr-3.6Sn is only 2.61%, indicating the optimal corrosion resistance in high temperature salt environments. The designed alloy Ti-5Al-4Zr-3.6Sn with optimized composition has great potential in practical applications.

3) For the three experiment α-Ti alloys with the same Bo_t value (3.487), both their σ_{UTS} and hot salt corrosion resistance are improved approximately linearly with increasing the Md_t value. The consideration of d-electron concept is an effective approach for the development of new α-Ti alloys with improved mechanical properties and hot salt corrosion resistance.

References

1 Christoph L, Manfred P. *Titanium and Titanium Alloys: Fundamentals and Applications*[M]. New Jersey: Wiley, 2003: 1

2 Xin S W, Liu X H, Zhang S Y *et al*. *Rare Metal Materials and Engineering*[J], 2023, 52(11): 3971

3 Liu Yanming, Jia Xinlu, Zhang Yisi *et al*. *Materials China*[J], 2023, 42(9): 699 (in Chinese)

4 Ezugwu E O, Wang Z M. *Journal of Materials Processing Technology*[J], 1997, 68(3): 262

5 Ghisi A, Mariani S. *International Journal of Fracture*[J], 2007, 146: 61

6 Liang C P, Gong H R. *International Journal of Hydrogen Energy*[J], 2010, 35(8): 3812

7 Joost W J, Ankem S, Kuklja M M. *Acta Materialia*[J], 2016, 105: 44

8 Matsugi K, Kashiwagi T, Choi Y B *et al*. *Materials Transactions*[J], 2011, 52(12): 2189

9 Ma X L, Matsugi K, Xu Z F *et al*. *Materials Transactions*[J], 2020, 61(4): 740

10 Morinaga M, Yukawa N, Maya T *et al*. *Sixth World Conference on Titanium*[C]. Cannes: TMS, 1988: 1601

11 Ma X L, Matsugi K, Xu Z F *et al*. *Materials Transactions*[J], 2019, 60(11): 2426

12 Matsugi K, Endo T, Choi Y B *et al*. *Materials Transactions*[J], 2010, 51(4): 740

13 Bae D, Jang S, Yukawa H *et al*. *Materials Transactions*[J], 2001, 42(6): 1112

14 Masahiko M, Junichi S, Masao M. *Light Metals*[J], 1992, 42(11): 614

15 Morishita M, Chikuda M, Ashida Y *et al*. *Materials Transactions*[J], 1991, 32(3): 264

16 Morinaga M. *Materials Transactions*[J], 2016, 57(3): 213

17 Jiang X J, Zhou Y K, Feng Z H *et al*. *Materials Science and Engineering A*[J], 2015, 639: 407

18 Laheurte P, Prima F, Eberhardt A *et al*. *Journal of the Mechanical Behavior of Biomedical Materials*[J], 2010, 3(8): 565

19 Adachi H, Tsukada M, Satoko C. *Journal of the Physical Society of Japan*[J], 1978, 45(4): 875

20 Matsugi K, Kishimoto H, Yamakawa D *et al*. *Materials Transactions*[J], 2015, 56(10): 1747

21 Murty B S, Kori S A, Chakraborty M. *International Materials Reviews*[J], 2002, 47(1): 3

22 Kazuhiro M, Kiyoshi S, Yong B C *et al*. *Journal of Japan Institute of Light Metals*[J], 2012, 62(12): 486

23 Wang J X, Ye X W, Li Y H *et al*. *Materials Science and Engineering A*[J], 2023, 869: 144788

24 Ma Jiakun, Zhang Miao, Feng Junning *et al*. *Titanium Industry Progress*[J], 2023, 40(6): 27 (in Chinese)

25 Hansen N. *Scripta Materialia*[J], 2004, 51(8): 801

26 Ronald W. *Armstrong Philosophical Transactions A*[J], 2015, 373(2038): 20140124

27 Yadav P, Saxena K. *Materials Today: Proceedings*[J], 2020, 60(2): 2546

28 Imayev V M, Gaisin R A, Gaisina E R *et al*. *Materials Science and Engineering A*[J], 2017, 696: 137

29 Zhao X L, Niinomi M, Nakai M *et al*. *Materials Science and Engineering C*[J], 2011, 31(7): 1436

30 Ritchie R O. *International Journal of Fracture*[J], 1999, 100: 55

31 Weck A, Wilkinson D S, Maire E. *Materials Science and Engineering A*[J], 2008, 488(1–2): 435

32 Myers J R, Bomberger H B, Froes F H. *Journal of Metals*[J], 1984, 36: 50

33 Dai J J, Zhu J Y, Chen C Z *et al*. *Journal of Alloys and Compounds*[J], 2016, 685: 784

耐腐蚀性能和拉伸性能提升的α型钛合金设计

马喜龙[1,2]，松木一弘[2]，尚志丰[1]，苏宏基[1]，贾博文[1]，聂国权[3]

(1. 石家庄铁道大学 材料科学与工程学院，河北 石家庄 050043)

(2. 广岛大学 工学部，日本 广岛 739-8527)

(3. 石家庄铁道大学 机械工程学院，河北 石家庄 050043)

摘　要：通过2个电子参数（结合次数Bo_t和d轨道能级Md_t）提出了新设计的α型钛（α-Ti）合金。新设计合金Ti-5Al-4Zr-3.6Sn、改性合金Ti-5Al-3Sn-1.9Zr和参考合金Ti-5Al-2.5Sn具有相同的Bo_t值（3.847）以及不同的Md_t值（2.430，2.426，2.422）。测试了3种α-Ti合金的极限抗拉伸强度（σ_{UTS}）、断裂应变（ε_f）和热盐腐蚀性能。3种α-Ti合金均采用冷坩埚悬浮熔炼技术进行制备。结果表明，3种合金样品均具有均匀的微观结构。在3种α-Ti合金中测量到的α单相晶粒尺寸约为600 μm。Ti-5Al-4Zr-3.6Sn合金的σ_{UTS}和ε_f值为801 MPa和16%，Ti-5Al-3Sn-1.9Zr合金的σ_{UTS}和ε_f值为708 MPa和15%，Ti-5Al-2.5Sn合金的σ_{UTS}和ε_f值为603 MPa和15%。热盐腐蚀测试进行28.8 ks后显示Ti-5Al-4Zr-3.6Sn、Ti-5Al-3Sn-1.9Zr和Ti-5Al-2.5Sn合金的失重率为2.61%、2.83%和3.10%。σ_{UTS}、ε_f和耐热盐腐蚀结果表明，新设计合金Ti-5Al-4Zr-3.6Sn是一种有实际应用潜力的钛合金材料。

关键词：合金设计；α型钛合金；冷坩埚悬浮熔炼；拉伸性能；热盐腐蚀测试

作者简介：马喜龙，男，1991年生，博士，石家庄铁道大学材料科学与工程学院，河北 石家庄 050043，电话：0311-87936067，E-mail：maxilong@stdu.edu.cn